Shock and Thermal Cycling Synergism Effects on Reliability of CBGA Assemblies

Reza Ghaffarian, Ph.D.
Jet Propulsion Laboratory
California Institute of Technology
Pasadena, California
818-354-2059
Reza. Ghaffarian@JPL.NASA.Gov

Abstract

Ball Grid Arrays (BGAs) are now packages of choice especially for higher I/O counts for commercial applications and are also being considered for use in military and aerospace. Thermal cycling characteristics of BGA assemblies have been widely reported including those by the JPL-led consortium. Thermal cycling represents the on-off environmental condition for most electronic products and therefore is key factor that defines reliability. As a results, much data available for accelerated thermal cycle conditions, but very limited data on vibration and shock representative of aerospace applications. Test vehicles with daisy chain plastic and ceramic BGAs (CBGAs) ranging from 256 to 625 I/O count were subjected to random vibration/shock representative of a spacecraft launch environment. The effect of board rigidity on behavior was also investigated by adding trips to or bonding of board to an Aluminum plate . This paper compares accelerated thermal cycles-to-failure data under four temperature ranges before and after thermal random vibration for CBGAs with 361 and 625 I/Os. Stress and strain projections by finite element analysis are also presented.

TABLE OF CONTENTS

1- ACCELERATED ENVIRONMENTAL TEST

Introduction

There are many purpose of performing accelerated environmental verification and testing program for electronics assemblies including:

- Qualification of design for in-service conditions
- Simulation of in-service test condition or to project life
- Definition of manufacturing variables and their effects
- Screening for manufacturing defects
- Demonstration of quality and reliability of a design
- Demonstration of suitability for the intended use

For electronics in commercial applications, commonly, thermal cycling tests are performed to simulate on/off condition. However, most electronic systems are exposed to other environments including mechanical fatigue and random vibration. Vibration occurs during transportation and mechanical fatigue by repeated use of key punching for portable electronics. Occasional high shock could occur due to accidental drops. Drop test and mechanical fatigue are started to be considered for qualification electronic assemblies especially for newer chip scale package assemblies.

In addition to much harsher thermal requirement for aerospace and military applications, generally assemblies are required to meet sever dynamic loads and vibration fatigue cycling. Therefore there is a strong need to understand behavior for such stress conditions. Very limited data are available for vibration and especially shock behavior of BGA assemblies. To understand behavior for space environment, several test vehicles with plastic and ceramic BGAs were subjected to dynamic testing representative of a launch, 3 minutes at 3 axis vibration/shock. Each test vehicle had four package types which were commercially available and had I/Os from 250 to 625 including both plastic and ceramic BGAs.

Synergism of thermal cycle representative of the following environmental conditions were considered:

- Prelaunch thermal cycling due to manufacturing, repair, screening, storage, and transportation
- Dynamic testing representative of launch environment which include sinusoidal vibration, transient vibration, pyroshock, and acoustic
- Thermal cycling representative of internal and external temperature change of a spacecraft

Effects of several variables were considered.

a) Thermal cycling before vibration/shock and after
b) Increase in rigidity of board by addition of thin rigid strips in one case and bonding to a rigid plate in another case
c) Change in thermal history condition by exposure to thermal cycles before vibration/shock

This paper presents experimental results as well as analyses for two CBGA assemblies (361 and 625 I/Os) subjected to either or both thermal cycling and vibration. Refer to the JPL BGA Packaging Guideline (Reference 1) for details on design, package daisy chain, board layout, manufacturing processes, inspection results, and thermal cycling behavior of ceramic and plastic package assemblies.

Literature Review

Cycles-to-failure after vibration of CBGAs and column (CCGA) were presented by M. Cole of IBM (Reference 2). Balls and columns were 90 Pb/10 Sn with 0.89 mm (.035 inch) in diameter for CBGA and for CCGA 0.5 mm (.02 inch) in diameter 2.2 mm (.050 or .087 inch) in height. Packages were assembled on FR-4 boards with single test specimens mounted on 110 x 90 mm board, clamped by screws at 101 x 75 mm locations. Mil-STD 810E were used to generate impact and vibration data for their test vehicle.

No failure of CBGAs and CCGAs was observed after vibration with heatsink of 73 g. CCGAs with heatsink weights of 100 and 150 grams failed whereas CBGAs did not. Cracks were induced in CBGAs in the eutectic solder either in package or board sites when subjected in 20-2000HZ with 7.73 grms. It was reported that for CBGAs, crack initiations were similar to those of accelerated thermal cycling (ATC), but with no deformation typically present in ATC. Also, thermal mismatch induce both shear and tensile, but vibration induce primarily tensile and not cause deformation.

It was observed that CBGA assemblies with heatsinks of lower weight that than 150 grams which were subjected to shock and vibration did not show any degradation in thermal fatigue life, no statistical differences between those with initial shock and vibration and those without any a priori test were observed.

In another study (Reference 3), CBGAs with 256 I/Os, 625, and 1089 I/Os were subjected to thermal cycling and vibration evaluation. The 1089 was fabricated with balls rather commonly supplied in column since they were used on metal matrix restraining core rather than polymeric board such as FR-4 . For restrained board with a CTE (6 ppm/°C) close to the ceramic package (7.2 ppm/°C), local mismatch between solder to package/board considered to play a primary role than global mismatch. Assemblies on restrained board were subjected to thermal cycling in the range of -55°C/125°C (a 5 °C/min ramp and a 30 minute dwell at each extreme) and they reported no failures to 1,500 cycles.

They also performed vibrations on three CBGAs at three levels:

- Level I was the military avionics equipment workmanship vibration level of Environmental Stress Screening (ESS)
- Level II was an enveloped subassembly based on several avionics programs
- Level III was the same as level II with power spectral density (PSD) increased by 3 dB.

Test results are listed in Table 1. All assemblies passed the level I whereas only CBGA with 254 I/O passed the Level II vibration. Finite element prediction for level I agreed with the experimental results, but for other levels had a mixed agreement.

2. TEST PROCEDURES

Test Vehicle

The test vehicles in this investigation included both plastic and ceramic packages on either FR-4 or polyimide printed circuit board (PWB) with six layers, 0.062 inch thick. Ceramic packages with 625 I/Os and 361 were included in our evaluation. Solder balls for CBGAs had high melt temperature composition (90Pb/10Sn) and about 0.035 inch diameters. The high melt balls were attached to the ceramic package with eutectic solder (63Sn/37Pb). At reflow, package side eutectic solder and the PWB side eutectic paste will be reflowed to provide the electro-mechanical interconnects.

The CBGAs had internal daisy chains which made a closed loop with daisy chains on the PWB enabling the monitoring of solder joint failure through continuous electrical monitoring. Daisy chains for CBGA 625 were in the ring form center to peripheral in order to identify failure sites with increased in thermal cycles. The first failure is known to occur from the peripheral ring in the corner solder joints with the maximum distance to neutral point (DNP). To improve assembly reliability, the supplier had removed package internal daisy chain connections among a few corner balls; excluding them from assembly failure detection during electrical monitoring. This means that cycles to first failure data cannot be directly correlated to package diagonal dimension which usually are assumed to be equal to the maximum DNP.

Thermal Cycling Conditions

Four different thermal cycle profiles were used. These were:

- Cycle A: The cycle A condition ranged from -30 to 100°C and had an increase/decrease heating rate of 2 to 5°C/min and dwell of about 20 minutes at the high temperature to assure near complete creeping. The duration of each cycle was 82 minutes.
- Cycle B: The Cycle B condition ranged from -55 to 100°C with long time duration. The heating and cooling rates were 2 to 5°C per minute with an oven dwell setting of 45 minutes at the two extreme temperatures. The duration of each cycle was 246 minutes.
- Cycle C: The cycle C condition ranged from -55 to 125 °C with 2-5°C/min heating/cooling rate. Dwell at extreme temperatures were at least 10 minutes with duration of 159 minutes for each cycle.
- Cycle D: The cycle D condition ranged from -55 to 125°C, the same as condition C, but with very high heating/cooling rate It could also be considered a thermal shock since it used a three region chamber: hot, ambient, and cold. Heating and cooling rates were nonlinear and varied between 10 to 15 °C/min. with dwells at extreme temperatures of about 20 minutes. The total cycle lasted approximately 68 minutes.

The criteria for an open solder joint specified in IPC-SM-785, Sect. 6.0, were used as guidelines to interpret electrical interruptions. Generally, once the first interruption was observed, there were many additional interruptions within 10% of the cycle life. This was especially true for ceramic packages.

Vibration

Three test vehicles with three levels of rigidity representing three loading conditions were stacked with spacers and subjected to random vibration. The bottom TV was bonded to an aluminum plate, the middle had center and edge stiffener strips, and the top had no stiffeners. The test vehicles were clamped from the two sides of PWB, the sides with no connectors as shown in Figure 1. The block of three stacked test vehicles were mounted on a very stiff thick Al plate on the shaker table with their natural frequencies well above the test vehicle assembly range.

Initially, a very low vibration spectrum was sweeped to determine natural frequencies for the test vehicle. The board were subjected to a vibration spectrum in the range of 200-2000HZ.

3. TEST RESULTS

Natural Frequency Measurement/Projection

Plots for natural frequencies were generated. A simplified finite element analysis was performed to predict natural frequencies and stress/strain condition at solder joint (Reference 4). Ten percent model damping was used for the random response calculation. Projections for the 1st, 2nd, and 3rd natural frequencies are compared to measured values as listed in Table 2.

Damage Induced for Thermal Cycling Alone

Both board and package interface cracking was observed with increasing number of cycles. Figure 2 shows typical failures for the two cycling conditions. Failure under the A conditions were generally from the PWB and for the D conditions from the package sites. Failure mechanism differences could be explained either by global or local stress conditions.

Modeling indicates that the high stress regions shifted from the board to the package themselves when stress conditions changed from the global to local. For the A cycling, with slow heat/cooling ramping, which allowed the system to reach uniform temperature, damages could indicate a global stress condition. For the D cycle with rapid heat/cooling, damages could indicate a local stress condition.

Damage Induced with a priori vibration

Damage induced by vibration was different in some cases as shown in Figures 3-4. Appearance of tensile deformation from the center of high balls as shown is significantly different from those observed for thermal cycling condition. Similarly to thermal cycle condition, damages were more dominant for the balls with higher DNPs, especially for the corner balls. However, additional microcracks in eutectic solder joints, different from the norm for thermal cycling, are induced by tensile and shear load during random vibration.

Cycles-to-failure for Thermal Cycling Alone

Figure 5 shows Weibull plots of cycles to first failures for CBGA 625 and CBGA 361 under four different thermal cycle conditions. To generate plots, cycles-to-failures for a population were ranked from low to high and failure distribution percentiles were approximated using median plotting position, $F_i = (i-0.3)/(n+0.4)$ (e.g., see Kapur,1977). Then, two-parameter Weibull distribution was used to characterize failure distribution. The Weibull cumulative failure distribution was used to fit cycles to failure data. The equation is

$$F(N) = 1 - \exp(-(N/No)^m)$$

where

F(N) is the cumulative failure distribution function
N is the number of thermal cycles
No is a scale parameter that commonly is referred to as characteristic life, and is the number of thermal cycles with 63.2% failure occurrence.
The m is the shape parameter and for a large m is approximately inversely proportional to the coefficient of variation (CV) by 1.2/CV; that is, as m increases, spread in cycles to failure decreases

This equation, in double logarithm format, results in a straight line. The slope of the line will define the Weibull shape parameter. The cycles-to-failure data in log-log were fitted to a straight line and the two Weibull parameters were calculated.

Synergism of Vibration and Thermal cycling

Cycles-to-failures for three assemblies with levels of rigidity and a priori vibration condition are shown in Table 3. Two test data for cycles-to-failure after vibration for the most sever condition, i.e. the test vehicles with no rigidity enhancement, were marked in Figure 5 for comparison only. It is difficult to draw a statistically meaningful conclusion because of insufficient sample size.

4. CONCLUSIONS

- A near-thermal shock in the range of -55°C to 125°C induced the most damage on CBGA assemblies, up to 50 percent reduction compared to a thermal cycle condition.
- Assemblies with three level rigidity passed a launch random vibration/shock condition. However, cycles-to-failures after vibration affected by the rigidity of the board, a significant reduction (>50%) for a less rigid and minimum reduction for highly rigid assemblies after vibration.
- Failures for thermal cycled CBGAs were either from board or package sites in the eutectic solder joints. Both tensile deformation in high melt balls and tensile and shear failures in eutectic solder were observed for assemblies subjected to vibration.

5. REFERENCES

1. Ghaffarian, R. "Ball Grid Array Packaging Guidelines," distributed by Interconnect Technology Research Institute (ITRI), August 1998, http://www.ITRI.org
2. Cole, M., Kastberg, E., Matin, G., "Shock and Vibration Limits for CBGA and CCGA", Surface Mount International Proceedings, 1996, pp.89-94
3. Marsico, J.W., AIL, private communications.
4. Pitarresi, J., University of New York at Binghamton, private communications.
5. Kapur, K.C., Lamberson, L.R., Reliability in Engineering Design, John Wiley & Sons, 1977

6. ACKNOWLEDGMENTS

The majority of research described in this publication was carried out by the Jet Propulsion Laboratory, California Institute of Technology, under a contract with the National Aeronautics and Space Administration.

I would like to acknowledge the in-kind contributions and cooperative efforts of JPL BGA Consortium on test vehicle design and assembly and those who contributed to the program. Also, thanks to Dr. James Pitarresi, University of New York at Binghamton for performing analytical modeling.

7- BIOGRAPHY

Dr. Reza Ghaffarian has nearly 20 years of industrial and academic experience in mechanical, materials, and manufacturing process engineering. At JPL, Quality Assurance Office, he supports research and development activities in SMT, BGA, and CSP technologies for infusion into NASA's missions. He has authored nearly 100 technical papers and numerous patentable innovations. He received his M.S. in 1979, Engineering Degree in 1980, and Ph.D. in 1982 in engineering from University of California at Los Angeles (UCLA).

Table 1 Vibration and thermal cycling for CBGAs

Vibration level	Duration (min)	Input level (grms)	Response (grms)	CBGA 256 I/O	CBGA 625 I/O	CBGA 1089 I/O
I	10	6.06	21	Pass (4/4)	Pass (2/2)	Pass (3/3)
II	60	12.8	37	Pass (4/4)	Pass (0/2)	Pass (0/3)
III	120	18.07	53	Pass (1/4)	NA	NA

Table 2 Measured and Finite Element Projection of Natural Frequencies and Stress/Strains for CBGA 361

TV Condition	Frequency Mode 1 (mode 2,3)	Amplitude (g^2/HZ)	Maximum Stress (Psi)	Maximum Strain (μStrain)
Measured Values for no Stiffener	356 (688,1700)	190	N/A	N/A
FEA for TV with no Stiffener	381 (594,795)	170	945	315
FEA for TV with Stiffeners	593 (820,1625)	43	558	185
FEA for TV bonded to Al Plate	3155 (3520,4700)	N/A	25	8

Table 3 Cycles-to-failures after random vibration

TV Condition	ID- Vibration (3 axes)& Thermal Cycle Type	Thermal Cycles to failure
No Stiffener Under Vibration	#4- Vib. + Cycle B #50- Vib. + Cycle B #34- Vib. + Cycle A	#4, Failed between 292 & 326 cycles #50- Failed at 400 cycles #34- No failure to 434
With Stiffeners	#33- Vib. + Cycle A #13- Vib. + Cycle A	#33, Failed between 292 and 326 cycles #13- Failed at 330 cycles
Bonded to Al Plate	#31- Vib.+ Cycle A	#31- No apparent change to virgin test vehicles

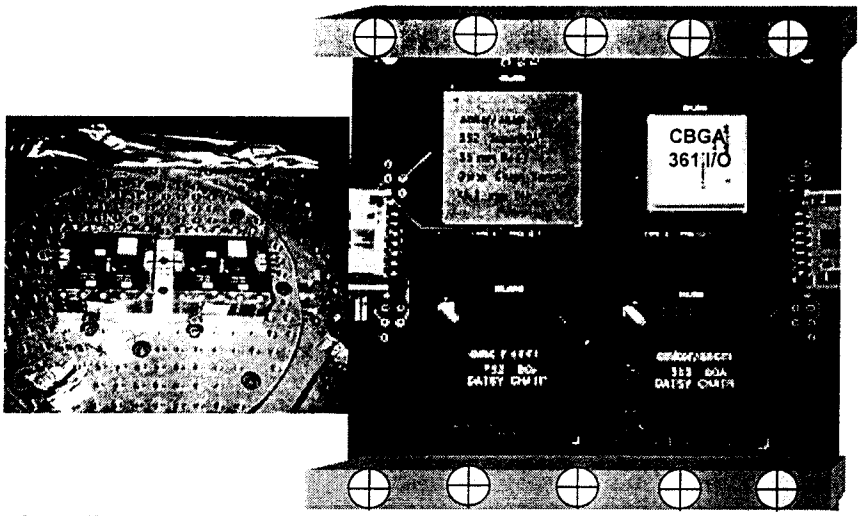

Figure 1 Photos of random vibration test set up, left photo shows two three-stack of test vehicle on vibration table and the right photo shows the enlarged test vehicle with the CBGA361 on the top right corner

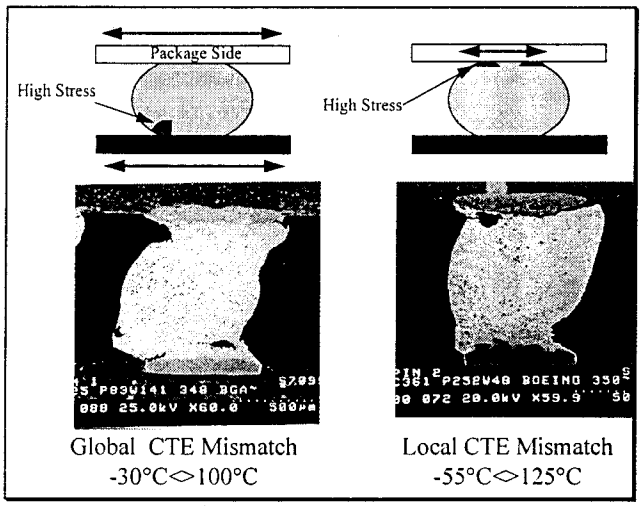

Figure 2 Cross-sections of failure sites for CBGA 625 after 350 cycles under A and CBGA 361 under D conditions

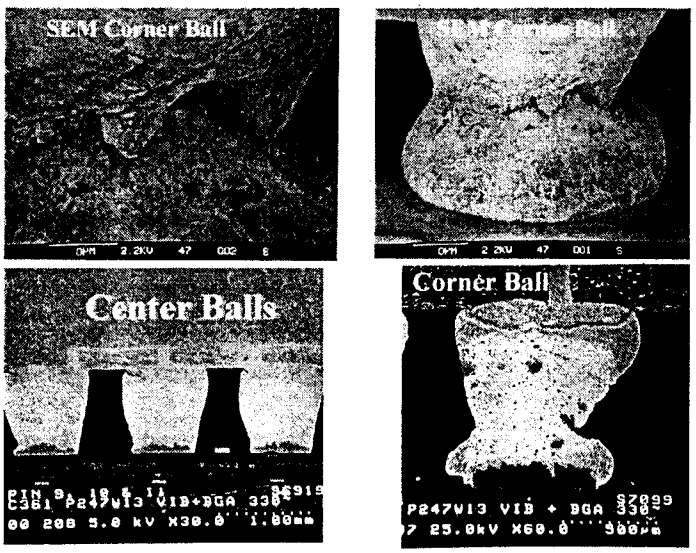

Figure 3 Thermally cycled samples after vibration. Note tensile failure for the corner ball and minimum damage for the center balls

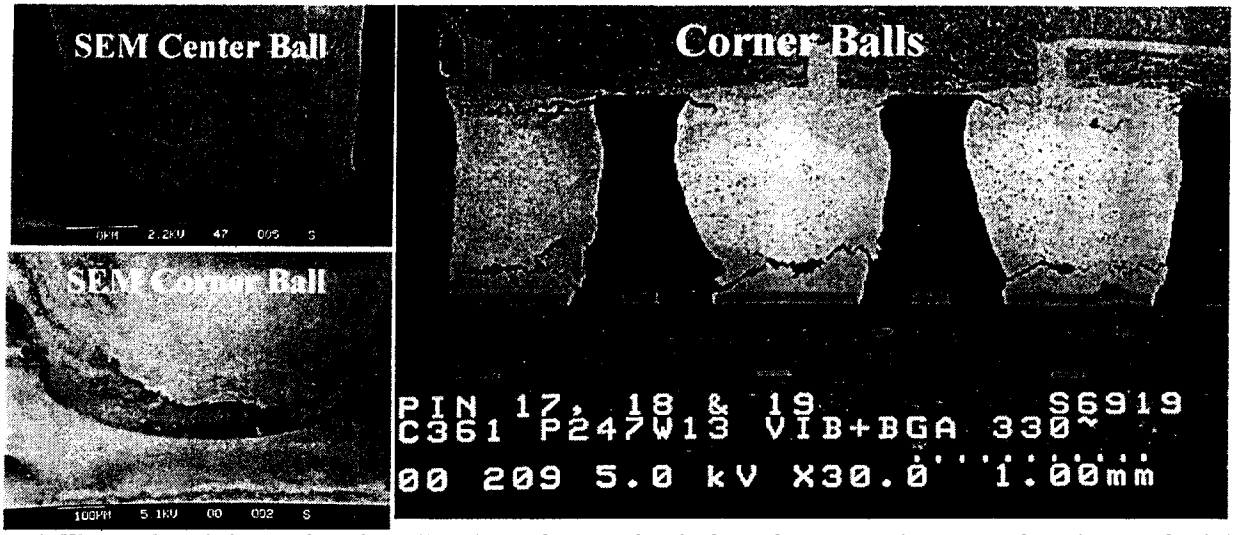

Figure 4 Thermal cycled samples after vibration. Note mechanical crack propagation at two locations and minimum damage at a center ball.

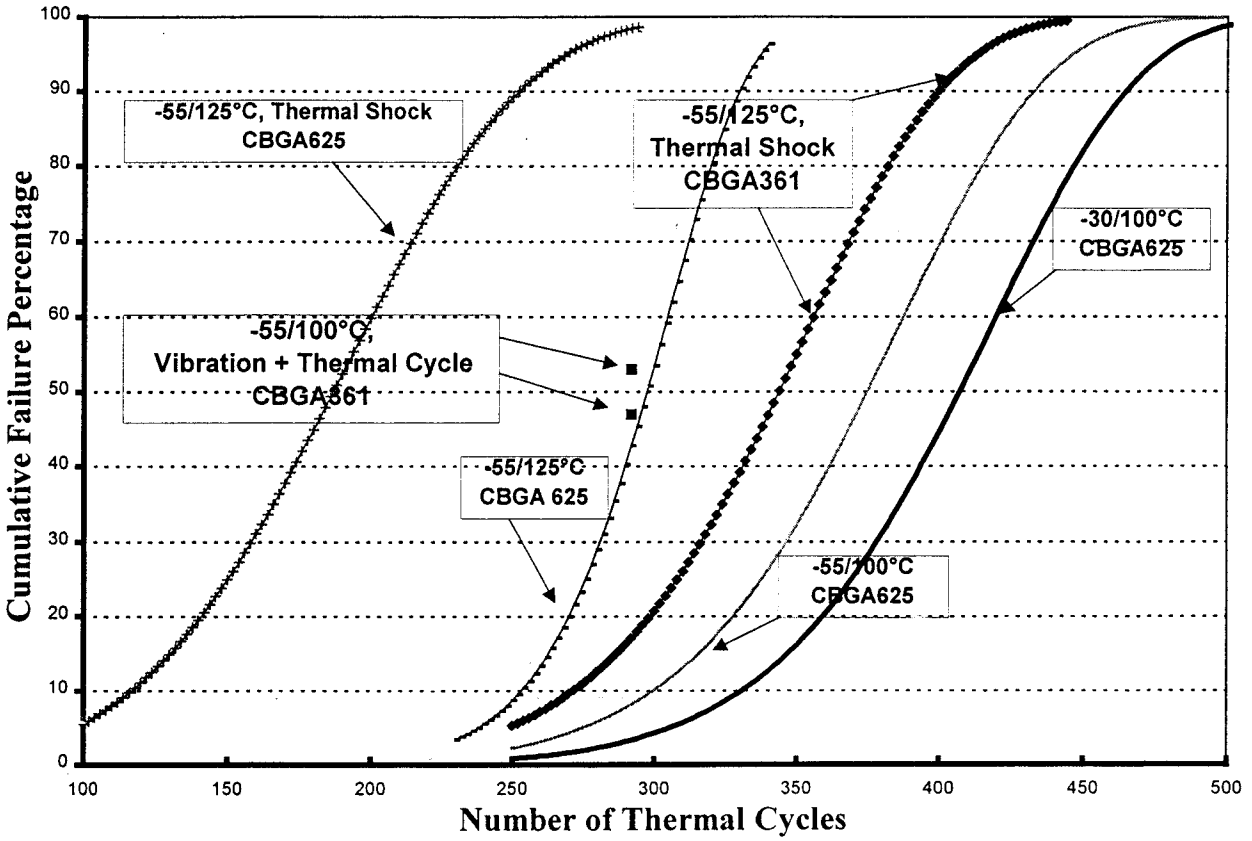

Figure 5 Cycles to failure data for two CBGAs under four thermal conditions with two assemblies with a priori vibration condition